INTERNATIONAL JOURNAL OF PHARMACEUTICAL SCIENCES
[ISSN: 0975-4725; CODEN(USA): IJPS00]
Journal Homepage: https://www.ijpsjournal.com

OPEN ACCESS

Research Paper

Quality By Design Based Preparation and Evaluation of Topical Nanoemulgel Loaded with A Model Drug for Management of Rheumatoid Arthritis

Mohammad Noufal*, Dr. Satheesha Babu B. K.

Government College of Pharmacy, Pharmaceutics department, Bangalore - 560027, Karnataka, India.

ARTICLE INFO

Published: 28 Aug 2026
Keywords:
Tofacitinib citrate, rheumatoid arthritis, Janus kinase inhibitors, nanoemulgel, Quality by Design, Pseudo-ternary phase, Risk assessment
DOI:
10.5281/zenodo.22144927

ABSTRACT

The present study aimed to develop and optimize a topical nanoemulgel containing tofacitinib citrate for localized management of rheumatoid arthritis, thereby reducing systemic exposure and safety concerns associated with oral Janus kinase inhibitors. Tofacitinib citrate was incorporated into an oil-in-water nanoemulsion using eucalyptus oil and a Tween 80-Transcutol®-P surfactant mixture, prepared by low-energy emulsification. A Quality by Design approach defined the target product profile and critical attributes, including particle size, polydispersity index, zeta potential, and entrapment efficiency. Pseudo-ternary phase diagrams confirmed stable nanoemulsion regions, and mixture design optimization identified oil and surfactant ratio as critical variables. The optimized nanoemulgel, formulated with Carbopol 934, exhibited nanosized droplets (<200 nm), low polydispersity, suitable zeta potential, and high drug entrapment. In vitro studies demonstrated sustained release up to 12 hours with consistent permeation flux, while stability testing confirmed formulation robustness. Overall, the developed nanoemulgel shows promise as an effective and safer topical alternative for rheumatoid arthritis management.

INTRODUCTION

Autoimmune diseases affect 8-10% of the global population, with rheumatoid arthritis (RA) being one of the most prevalent and disabling forms (Scott, 1987). In 2019, RA impacted nearly 18 million individuals worldwide, with higher prevalence among women and older adults (Radu, 2021; Kumari et al., 2024). The disease is marked by chronic synovial inflammation, autoantibody production, and progressive joint destruction, often accompanied by systemic complications such as cardiovascular and pulmonary disease, which increase morbidity and mortality.

***Corresponding Author:** Mohammad Noufal
Address: *Government College of Pharmacy, Pharmaceutics department, Bangalore - 560027, Karnataka, India.*
Email ✉: mohammadnoufal614@gmail.com
Relevant conflicts of interest/financial disclosures: The authors declare that the research was conducted in the absence of any commercial or financial relationships that could be construed as a potential conflict of interest.

Despite therapeutic advances, the global burden of RA continues to rise, as shown by increasing incidence and disability-adjusted life years (Guo et al., 2016). Conventional synthetic DMARDs (csDMARDs), particularly methotrexate, remain the first-line therapy due to efficacy and affordability (Tanaka, 2016; Kekane, 2020), but long-term systemic use is associated with adverse effects and variable response (Glynn, 1968). Biologic DMARDs targeting inflammatory mediators such as TNF-α and IL-6 have improved outcomes but are limited by cost, parenteral administration, and infection risk (Karnam, 2024). More recently, Janus kinase (JAK) inhibitors have emerged as effective oral therapies, though systemic safety concerns-including thromboembolic and cardiovascular risks which restrict their widespread use (Zou, 2023).

These limitations highlight the need for localized drug-delivery strategies that maintain efficacy while reducing systemic exposure. Topical nanoemulgels offer enhanced dermal penetration, sustained release, and prolonged drug residence at inflamed joints (Takanashi, 2024; Valrmathy, 2024). Applying Quality by Design (QbD) principles enables systematic optimization of formulation variables, ensuring reproducibility, stability, and regulatory compliance (Pramod et al., 2016). Accordingly, this study focuses on the development and evaluation of a QbD-optimized topical nanoemulgel of tofacitinib citrate as a safer, site-specific alternative to systemic JAK inhibitor therapy (Sinha et al., 2024).

2.0 MATERIALS AND METHODS:

2.1 Materials: Tofacitinib citrate was procured from Optimus Drugs Pvt. Ltd, Hyderabad. The excipients used in the formulation included Eucalyptus oil (Ganesh Oil Distillery, Ooty), Tween-80 (Thomas Baker Chemicals Pvt. Ltd, Mumbai), Transcutol®-P (Gattefosse SAS, Mumbai) and Carbopol-934 (Corel Pharma Chem, Gujarat). Methanol and Triethanolamine were obtained from Spectrochem Pvt. Ltd, Bangalore. Preservatives such as Methyl Paraben and Propyl Paraben were purchased from Hi-Media Laboratories Pvt. Ltd, Thane. Sodium hydroxide was supplied by Spectrochem Pvt. Ltd, Bangalore, while Potassium dihydrogen phosphate was obtained from Central Drug House (P) Ltd, Gujarat. All chemicals and reagents used were of analytical grade.

2.2 Physicochemical Characterization of the Drug Substance: Preformulation studies were conducted to evaluate the fundamental physicochemical characteristics of Tofacitinib Citrate prior to formulation development.

2.2.1 Organoleptic Properties: The organoleptic characteristics of Tofacitinib Citrate namely its colour, physical form and odour were assessed through direct visual and olfactory examination under ambient laboratory conditions.

2.2.2 Determination of Melting Point: A small quantity of Tofacitinib Citrate was introduced into a dry, thin-walled capillary tube (approximately 8-10 cm in length and 1 mm in internal diameter, sealed at one end). The tube was placed in a digital melting point apparatus and gradually heated. The temperature at which the sample transitioned from solid to liquid was recorded as the melting point. This procedure was repeated three times to ensure reproducibility and the average value was calculated.

2.2.3 Determination of Solubility: Weigh an accurately measured sample into a stoppered test tube or small flask, add a known volume of the chosen solvent, cap and mix thoroughly to disperse the solid, then allow the mixture to equilibrate at the test temperature for about 15 min. Inspect visually for complete dissolution, turbidity, phase

separation, or undissolved residue. Record solvent, temperature, sample mass, solvent volume, mixing and equilibration times and classify the outcome qualitatively (insoluble, sparingly soluble, slightly soluble, soluble, freely soluble, or miscible).

2.3 Screening of Oil, Surfactants and Co-surfactants:

2.3.1 Solubility of Tofacitinib Citrate in oils, surfactant and co-surfactant: To identify the optimal oil, surfactant and co-surfactant phase for nanoemulsion formulation, the solubility of Tofacitinib citrate was assessed using the shake flask method. Five oils (olive oil, IPM, eucalyptus oil, oleic acid, peppermint oil), three surfactants (Tween-20, Tween-80, Poloxamer-188) and two co-surfactants (Transcutol®-P, PEG-400) were selected from literature. Excess drug was added to 2 ml of each excipient, vortexed for 30 sec and shaken at 120 rpm in a 37 ± 0.5 °C water bath for 72 h. Samples were centrifuged at 3000 rpm for 15 min and the supernatant filtered (0.45 µm). Filtrates were diluted with methanol and analyzed spectrophotometrically at 286 nm. Experiments were performed in triplicate and mean solubility values recorded. All excipients were GRAS-certified and suitable for topical use (Patel PA, 2019; Jaydip, 2020).

2.3.2 Emulsification Efficiency Test: To identify the most suitable surfactant system for emulsifying the selected oil phase, various surfactants and co-surfactants were evaluated based on their emulsification efficiency and ability to form stable nanoemulsions. For screening, 1 ml of eucalyptus oil was mixed with 1 ml of Smix of different ratio (1:1, 1:2, 2:1 etc) and vortexed for 60 seconds to ensure uniform mixing. From the resulting isotropic mixture, 1 ml was accurately weighed and added dropwise to the 100 ml of distilled water. To assess emulsification efficiency, observe the emulsification time, clarity and phase separation and % Transmittance is observed using UV- VISIBLE Spectrophotometer at the wavelength 650 nm. The Smix ratio having best emulsification efficiency was selected for plotting psuedoternary phase diagram (Aboul et al, 2017).

2.4 Compatibility Studies

Compatibility studies were conducted to evaluate potential physicochemical interactions between Tofacitinib citrate and the selected excipients used in the nanoemulsion formulation namely eucalyptus oil, Tween 80 and Transcutol®-P. These studies were essential to ensure formulation stability, drug integrity and performance over time (Daware et al, 2025; Sivapriya 2023).

2.4.1 Fourier Transforms Infrared Spectroscopy (FT-IR): It was employed to assess chemical compatibility between the drug and excipients. FT-IR spectra were recorded using a Bruker Alpha II spectrometer across the spectral range of 4000-400 cm^{-1}. Samples analysed included pure Tofacitinib citrate, individual excipients and the optimized nanoemulgel formulation. The spectra were interpreted for any appearance, disappearance, or shifting of characteristic peaks, which could indicate potential interactions or incompatibilities.

2.4.2 Differential Scanning Calorimetry (DSC): Differential Scanning Calorimetry (DSC) was employed to investigate the thermal behaviour of the formulation. Approximately 1–3 mg or ml of each sample was accurately weighed and sealed in aluminium pans using a Shimadzu crimper. A similarly sealed empty pan served as the reference. The analysis was conducted under a nitrogen atmosphere, which acted as the purging gas, at a scanning rate of 10 °C per minute. The temperature ranges for the study extended from 20 °C to 300 °C, with heat runs performed from 3 °C to 320 °C. This thermal profiling provided insights into the formulation's phase transitions,

stability and compatibility of excipients with the active pharmaceutical ingredient.

2.5 Construction of Pseudo Ternary Phase Diagram:

To delineate the nanoemulsion region and identify optimal component ratios, pseudo ternary phase diagrams were constructed using eucalyptus oil as the oil phase and Tween 80 and Transcutol®-P as the surfactant and co-surfactant, respectively. Surfactant-to-co-surfactant mixtures (Smix) were optimized from emulsification efficiency test. Aqueous titration was carried out with Smix blended with the oil phase in varying proportions ranging from 1:9 to 9:1. The mixtures were vortexed for 2–3 minutes to ensure homogeneity. Then slowly drop-by-drop water is added to the mixture of oil and Smix until change in phase is observed. Samples appearing transparent or slightly bluish were considered indicative of nanoemulsion formation. The phase diagrams were plotted to highlight the nanoemulsion zones and each experiment was performed in triplicate to ensure reproducibility. Chemix School software was used to plot the diagram (Mendes et al, 2016).

2.6 Formulation Development using Quality by Design (QbD)

2.6.1 Setting Quality Target Product Profile (QTPP) and Critical Quality Attributes (CQAs): The development of a nanoemulgel formulation for topical delivery of Tofacitinib citrate was guided by the principles of Quality by Design (QbD), beginning with the establishment of a Quality Target Product Profile (QTPP). The QTPP outlines the desired characteristics of the final product that align with therapeutic goals and regulatory expectations. For topical nanoemulgel systems, key attributes include optimal particle size for enhanced skin permeation, physical stability (absence of phase separation) and effective drug release to ensure local action. These attributes were selected to ensure patient-centric performance, safety and efficacy. Based on the QTPP, Critical Quality Attributes (CQAs) were identified-parameters that directly influence product quality and must be controlled throughout development. Any variation in QTPP may significantly impact CQAs, thereby affecting the overall performance of the formulation. This systematic approach ensures that the formulation remains robust, reproducible and compliant with its intended use (Vohra et al, 2017).

2.6.2 Risk Assessment and Process Understanding:

In the context of Quality by Design (QbD), a systematic evaluation of formulation components and variables was undertaken to identify factors that significantly influence the therapeutic performance of the nanoemulgel containing Tofacitinib citrate. To explore potential interactions between the drug and selected excipients-eucalyptus oil, Tween 80 and Transcutol®-P -multiple unit operations were considered during preliminary development. A structured risk assessment approach was employed to anticipate possible formulation failures that could impact critical quality attributes (CQAs). Using Failure mode effective analysis (FMEA) diagram was constructed to facilitate visualization of probable root causes and minor contributing factors affecting CQAs such as Particle size, PDI, Zeta potential and entrapment efficiency. This tool enabled efficient categorization of risks under domains such as material attributes, process parameters and environmental conditions, thereby guiding the selection of variables for further optimization.

2.6.3 Experimental Design: A mixture design approach was used to optimize the nanoemulsion, ideal for systems where responses depend on component proportions. The formulation included

oil (15–20%), Smix (25–30%) and water (50–55%), selected from pseudo-ternary plot screening to ensure stability and coverage of the nanoemulsion region. A Simplex Lattice Design with 6 mixture points and 2 replications (8 runs) systematically explored component interactions. Responses measured particle size, PDI, zeta potential and entrapment efficiency assessed quality, stability and drug delivery potential. This design provided a robust statistical framework to optimize component ratios and develop a stable, efficient nanoemulsion (Cornell, 2011).

2.7 Formulation of Nanoemulgel (NEG)

Step 01- Preparation of Nanoemulsion(NE): Tofacitinib citrate was incorporated into a nanoemulsion using a low-energy emulsification technique. The drug (0.1% w/w) was dissolved in a pre-optimized oil–surfactant–co-surfactant mixture selected from the nanoemulsion region of the pseudo-ternary phase diagram. The oil phase was prepared by mixing the oil, surfactant and co-surfactant under magnetic stirring until a homogeneous blend was obtained. Distilled water was then added slowly to the oil phase at room temperature without the application of heat or high-shear forces. The aqueous phase was introduced dropwise at a controlled rate (approximately 50–60 drops per minute) under continuous stirring at 250–300 rpm. Addition of water was continued until a clear and transparent nanoemulsion was formed, indicating successful emulsification. The low-energy method was selected to ensure drug stability, minimize mechanical stress and support scalability and energy-efficient processing.

Step 02- Incorporation of Nanoemulsion(NE) into Gel base: The gel base was prepared by dispersing Carbopol 934 (0.5% w/w) in purified water under continuous stirring using an overhead stirrer at 2000 rpm for 5 min. Methyl paraben and propyl paraben were incorporated at permissible concentrations by dissolving them in the aqueous phase prior to gel formation. The dispersion was neutralized with triethanolamine to obtain the desired pH and gel consistency suitable for topical application. The optimized drug-loaded nanoemulsion was then incorporated into the gel base in a 1:1 ratio. Mixing was carried out gently using a magnetic stirrer until a smooth and homogeneous nanoemulgel was obtained (Kumar et al; Jamadra, 2017; Singh, 2005).

2.8 Evaluation of Nanoemulsion (NE) Formulation:

2.8.1 Organoleptic Characteristics: The nanoemulgel was assessed visually for appearance, colour, odour, texture and clarity to ensure acceptable aesthetic and sensory characteristics for topical use.

2.8.2 Particle Size and Polydispersity Index (PDI): The particle size and PDI of the nanoemulsion were measured using Dynamic Light Scattering (DLS) with a Zetasizer Nano ZS (Malvern Instruments, UK). Prior to analysis, samples were diluted tenfold with distilled water to minimize multiple scattering effects. Measurements were conducted at 25 °C in triplicate (Sharma, 1997).

2.8.3 Zeta Potential: Zeta potential of the nanoemulsion was measured using a Zetasizer to assess surface charge and colloidal stability. Diluted samples were analysed at 25 °C, with values ≥ ±30 mV considered indicative of adequate electrostatic stability (Trotta, 2003).

2.8.4 Entrapment Efficiency: Entrapment efficiency was determined using an indirect centrifugation method. It is assessed by centrifuging the nanoemulsion at 10,000 rpm for 30 minutes to separate the unentrapped drug. The

supernatant was collected and analysed using UV-VISIBLE-visible spectrophotometry at the λmax of Tofacitinib Citrate.

Entrapment efficiency was calculated using the formula:

$$\% \text{ Entrapment efficiency} = \frac{\text{Total drug} - \text{unentrapped drug}}{\text{Total drug}} \times 100$$

This parameter reflects the proportion of drug successfully encapsulated within the nanoemulsion droplets, which is critical for therapeutic performance (Jain, 2016).

2.8.5 Drug Content: Drug content was determined by dissolving a known quantity of nanoemulgel in methanol, followed by sonication to ensure complete drug release. The solution was filtered and analysed spectrophotometrically at the 286 nm. The concentration was calculated using a standard calibration curve and drug content was expressed as a percentage of the theoretical amount (Garg et al, 2022). This confirms uniform drug distribution throughout the formulation. It is calculated using formula;

$$\% \text{ Drug Content} = \frac{\text{Actual drug Content}}{\text{Theoretical loading}} \times 100$$

2.8.6 Thermodynamic Stability Study: Thermodynamic stability was evaluated through heating-cooling cycles to assess the formulation's resistance to temperature stress. The nanoemulsion was subjected to three cycles, each consisting of storage at 4 °C and 45 °C for 48 hours. After each cycle, formulations were inspected visually for signs of phase separation, turbidity, creaming, or cracking. Formulations that remained clear and homogeneous were considered thermodynamically stable and suitable for further development (Ghogare, 2022).

2.8.7 Scanning Electron Microscopy (SEM): Surface morphology and droplet shape of the nanoemulsion and nanoemulgel were examined using Scanning Electron Microscopy (SEM). A small amount of sample was mounted on an aluminium stub, air-dried and coated with a thin layer of gold using a sputter coater. The sample was then observed under SEM at appropriate magnifications. SEM images provided visual confirmation of spherical droplets with smooth surfaces and uniform distribution, supporting the physical characterization of the nanoemulsion (Bhardwaj, 2014).

2.8.8 Percent Transmittance (%T): The optical clarity of the optimized nanoemulsion was evaluated by measuring percent transmittance (%T) using a UV- VISIBLE-visible spectrophotometer. A small aliquot of the nanoemulsion was diluted appropriately with distilled water and scanned at 650 nm, a wavelength commonly used to assess turbidity and light scattering. A high %T value (typically above 90%) indicates a transparent system with uniformly dispersed droplets in the nanometre range, confirming successful emulsification and physical stability. This parameter was particularly useful for distinguishing nanoemulsions from coarse emulsions, which exhibit lower transmittance due to larger droplet sizes and increased light scattering (Nayak, 2010).

2.9 Evaluation of Nanoemulgel (NEG) loaded with optimized Nanoemulsion:

2.9.1 Homogeneity: The emulgel formulations were visually examined for uniformity, smooth texture and absence of lumps or phase separation to confirm proper integration of the gel and emulsion phases

2.9.2 pH Measurement: pH of the formulation was determined using digital pH meter. pH meter

electrode was washed by distilled water and then dipped into the formulation to measure pH and this process was performed in triplicate.

2.9.3 Spreadability Test: A 0.5 g sample of formulation was placed between two standard-sized glass slides and left undisturbed for approximately 5 minutes, allowing the material to spread naturally until no further increase in diameter was observed. The diameter of the resulting spread circle was measured in centimeters and used as an indicator of spreadability. The values reported represent the mean of three independent measurements (Basha, 2011).

2.9.4 Viscosity: Viscosity was measured using a Brookfield viscometer equipped with a T-bar spindle and Helipath stand at ±37 °C. Readings were recorded at various spindle speeds (50rpm) to evaluate the rheological behaviour of the emulgel. Viscosity affects drug release, retention time and spreadability (Patel 2011).

2.9.5 Drug Content: Drug content was determined by dissolving 1 g of emulgel in 15 ml of methanol. The mixture was vortexed for 5 minutes at 5000 rpm and sonicated for 15 minutes to ensure complete solubilization. After appropriate dilution, the absorbance was measured at 286 nm using a UV- VISIBLE-visible spectrophotometer (UV- VISIBLE-1800, Shimadzu, Japan), with methanol as the blank. Drug concentration was calculated using a standard calibration curve (Ramesh, 2010).

2.9.6 *In Vitro* Drug Release Study: *In vitro* diffusion studies were performed using a modified USP Dissolution Apparatus II. This approach was selected to simulate topical drug diffusion through a semipermeable barrier under controlled conditions.

Membrane Preparation: A fresh egg membrane was used as the semipermeable barrier due to its natural porosity and compatibility with topical formulations. The membrane was carefully separated from the egg shell, thoroughly washed with distilled water to remove residual albumin and soaked overnight in 2M hydrochloric acid to ensure uniform hydration and pliability.

Sample Holder Assembly: A cylindrical glass tube, approximately 5 cm in length and 1.5 cm in diameter, was used as the sample holder. The nanoemulgel formulation equivalent to 2 mg drug was loaded into the tube and one end was sealed with the prepared egg membrane. The membrane was secured using non-reactive thread to prevent leakage and ensure tight sealing. The tube was then vertically tied to the paddle shaft of the dissolution apparatus, with the membrane end facing downward and immersed upto 1 cm in the dissolution medium.

Diffusion Conditions: The diffusion medium consisted of 100 ml of phosphate buffer at pH 6.8, maintained at 37 ± 0.5°C to mimic physiological conditions. The paddle rotation speed was set at 75 rpm. Samples were withdrawn at predetermined intervals and analysed spectrophotometrically at 286 nm. The release profile was used to assess the rate and extent of drug diffusion from the emulgel matrix (Dash S et al, 2010).

2.9.7 Drug Release Kinetics: To analyse the *in vitro* drug release behaviour, various mathematical models were employed to assess the release kinetics. The zero-order model (Equation 1) describes a system in which the drug is released at a constant rate, independent of its concentration. Conversely, the first-order model (Equation 2) illustrates a release pattern where the rate is proportional to the concentration of the drug remaining in the formulation. The Higuchi model (Equation 3) explains drug release from an insoluble matrix, where the release follows a

diffusion-controlled mechanism and is proportional to the square root of time, aligning with Fick's law of diffusion. The Korsmeyer-Peppas model (Equation 4) is used to characterize the drug release mechanism from polymer-based systems by establishing a relationship between the fraction of drug released and time.

Zero order kinetics:

$C = k_0 t$ (1)

where, C is the concentration of drug at time t, t is the time and k0 is zero-order rate constant expressed in units of concentration/time

First order kinetics:

$\text{Log } C_0 - \text{Log } C = k_1 t/2.303$ (2)

where, C_0 is the initial concentration of drug and k_1 is the first order rate constant.

Higuchi model:

$C = K_H \sqrt{t}$ (3)

where, K_H is the constant reflecting the design variables of the system.

Korsmeyer-Peppas model:

$Mt/M\infty = K_{KP} t^n$ (4)

Where, $Mt/M\infty$ is the fraction of drug released at time t, K_{KP} is the rate constant and n is the release exponent.

The data obtained is plotted between log time and log percentage cumulative drug release.

2.9.8. In vitro Permeability study:

Steady-State Flux: Steady-state flux is the constant rate at which drug passes through a membrane or is released from a formulation per unit area once steady conditions are reached. Experimentally in *in vitro* release or permeation tests it is the slope of the linear portion of cumulative amount versus time divided by the exposed area, expressed as mass per area per time.

Steady-state flux = Slope / Area

Permeability Coefficient: Permeability coefficient quantifies how fast a drug crosses a barrier (membrane or tissue) per unit concentration difference and area; experimentally the apparent permeability in *in vitro* study is calculated from the steady flux by dose, expressed as cm/s or cm/hr.

Permeability Coefficient = Steady-state flux / Dose

2.10 Stability Studies

The optimized tofacitinib citrate nanoemulgel was subjected to accelerated stability testing to evaluate its physical and chemical stability. The formulation was filled into tightly sealed glass vials and stored under accelerated conditions (40 ± 2 °C / 75 ± 5% RH) for 30 days. Controlled humidity was maintained using a saturated sodium chloride solution.

Samples were withdrawn at 0, 7, 15 and 30 days and evaluated for physical appearance, phase separation and drug content. The study was performed to assess formulation stability and to support storage condition and shelf-life recommendations (ICH guidelines, 2003).

3.0 RESULTS AND DISCUSSION:

3.1 Preformulation studies:

TCN was confirmed as a white to off-white powder with a melting point of 198°C which is further confirmed by DSC, consistent with literature values and indicative of its purity. Its solubility profile revealed high solubility in DMSO and methanol, moderate solubility in phosphate buffer (pH 6.8) and poor solubility in ethanol.

3.2 Screening of oils, surfactants and co-surfactants:

Among screened oils, eucalyptus oil exhibited the highest solubility for TCN (28.64 µg/mL) (Figure 1), followed by peppermint and oleic acid. Tween

80 emerged as the most effective surfactant (25.76 µg/mL) (Figure 2), while Transcutol®-P showed superior solubilizing capacity among co-surfactants (33.12 µg/mL) (Figure 3). These selections were guided by solubility and emulsification efficiency, ensuring optimal drug loading and nanoemulsion stability.

Tofacitinib citrate showed the highest solubility in eucalyptus oil, attributed to terpene components such as cineole that enable favorable lipophilic and hydrogen-bonding interactions. Other oils demonstrated lower solubility due to higher viscosity, esterified structures, or long-chain fatty acids that limit drug–excipient interactions. Tween 80 provided greater solubilization than Tween 20 and poloxamer, likely due to its longer oleate chain and improved micellar incorporation. Transcutol® P exhibited superior solubility compared to PEG 400 because of its amphiphilic nature and strong solvent capacity, whereas the higher hydrophilicity of PEG 400 restricted effective drug interaction.

3.3 Emulsification efficiency and phase diagram:

The Smix ratio of 3:1 (Figure 4) demonstrated the highest transmittance (92.2%) and rapid emulsification (<1 min) without phase separation, indicating superior clarity and stability. Pseudo-ternary phase diagrams confirmed the existence of a broad nanoemulsion region, supporting formulation robustness. These findings were critical in defining the design space for Quality by Design (QbD) optimization (Table 7 & 9).

This ratio offered an optimal surfactant–co-surfactant balance, effectively reducing interfacial tension and enabling efficient droplet formation, which resulted in rapid emulsification and high transmittance indicative of small droplet size and good clarity.

3.4 Compatibility studies:

3.4.1 FTIR Analysis: FTIR analysis of TCN and its physical mixtures with selected excipients showed retention of key characteristic peaks corresponding to amide, hydroxyl and aromatic functional groups (Table 8). The absence of peak shifts or disappearance indicates no chemical interaction, confirming the structural integrity and compatibility of the drug with the excipients used in the nanoemulgel formulation.

3.4.2 DSC Analysis: DSC thermograms showed a sharp melting endotherm for pure TCN that was retained in the drug–excipient mixture without significant shift or broadening, indicating thermal stability, absence of interaction and preserved formulation integrity. (Figure 7 & 8).

3.5 Formulation development using QbD:

A QbD approach was used to develop the TCN nanoemulgel for effective topical delivery and sustained release. The QTPP defined key targets, including clear appearance, efficient skin penetration and >60% drug release over 12 h (Table 10). CQAs such as particle size, PDI, zeta potential, viscosity and entrapment efficiency were identified, while FMEA highlighted the oil phase and surfactant system as high-risk factors affecting formulation performance (Table 11).

3.6 Initial risk assessment:

FMEA highlighted the oil phase and surfactant system as major risk factors affecting CQAs, with the aqueous phase and storage conditions being secondary. Oil selection influences viscosity, solubility, entrapment and stability, while surfactant type and Smix ratio control interfacial tension, droplet size, PDI, zeta potential and drug release. The aqueous phase mainly impacts pH and zeta potential, whereas storage conditions may induce instability. Accordingly, optimization prioritized oil screening, Smix optimization, aqueous phase control, droplet size regulation and targeted stability studies.

3.7 Formulation and optimization of TCN loaded nanoemulsion:

A TCN nanoemulsion was prepared using a low-energy method and optimized through a Simplex Lattice Mixture Design evaluating oil, Smix and water. Eucalyptus oil, Tween 80 and Transcutol®-P were selected and their effects on particle size, PDI, zeta potential and entrapment efficiency were optimized. The optimized nanoemulsion was incorporated into a Carbopol 934 gel to obtain the final nanoemulgel for topical rheumatoid arthritis treatment.

3.8 Evaluation of TCN loaded NE:

3.8.1 Physical Characterization: The formulation appeared yellowish-transparent with no phase separation, high optical clarity (% transmittance 98 ± 2%) and near-complete drug loading (drug content 97 ± 1.5%). These results indicate a physically homogenous, optically clear system with uniform drug distribution and good assay accuracy, the sample demonstrates suitable quality for further optimization and stability studies (Table 16).

3.8.2 Response Analysis:

3.8.2.1 Particle size: The fitted mixture model predicted particle size as:

PS = −464.140*Oil + 154.340*Smix + 38.140*Water + 9.040*(Oil×Smix) + 6.400*(Oil×Water) + 2.720*(Smix×Water).

A negative oil coefficient indicates that increasing oil reduces particle size by improving solubilization and interfacial curvature, while excess Smix and water slightly increase size due to interfacial thickening and altered packing. Positive interaction terms suggest partial antagonism when components are combined. Minimum particle size is achieved in an oil-rich region with only sufficient Smix for stability, as indicated by response surface optimization. The response analysed by quadratic mixture design with model $F = 532.40$, $p < 0.05$, $R^2 = 0.9992$, Adj $R^2 = 0.9974$ indicating significant response. The actual and predicted values of particle size were correlated as shown in the figure 10.

3.8.2.2 Polydispersity index (PDI): The fitted mixture model predicted PDI as:

PDI = 1.45640*Oil + 0.73760*Smix − 0.57440*Water + small interaction terms.

A positive oil coefficient indicates that higher oil content broadens PDI due to formation of multiple droplet populations and incomplete interfacial coverage, while excess Smix also increases PDI because of micelle formation and uneven interfacial packing. In contrast, increased water content narrows the size distribution by diluting free surfactant and improving droplet uniformity. Interaction effects were minimal, indicating no strong synergistic influence within the studied range. The response analysed by quadratic mixture design with model $F = 265.26$, $p < 0.05$, $R^2 = 0.9985$, Adj $R^2 = 0.9947$ indicating significant response. The actual and predicted values of Polydispersity index were correlated as shown in the figure 12.

3.8.2.3 Zeta potential: The fitted mixture model predicted Zeta potential as:

Zeta (mV) = 34.82250*Oil − 37.72750*Smix − 22.07250*Water + small interactions.

A positive oil coefficient indicates that increasing oil content shifts zeta potential toward less negative values by modifying interfacial composition and masking charged groups. In contrast, higher Smix and water levels drive zeta potential more negative due to increased surfactant adsorption, ionization and double-layer formation at the interface. Interaction effects were minor, suggesting only limited modulation of these primary trends through combined component changes. The response analysed by quadratic

mixture design with model F = 10.11, $p < 0.05$, R^2 = 0.9309, Adj R^2 = 0.8388 indicating significant response. The actual and predicted values of zeta potential were correlated as shown in the figure 14.

3.8.2.4 Entrapment efficiency (%EE): The fitted mixture model predicted Zeta potential as:
%EE = 12.94467·Oil − 7.59800*Smix + 1.78867*Water − 0.52800*(Oil×Smix).
A positive oil coefficient indicates that higher oil content increases %EE by providing greater solubilization and lipid volume, while excess Smix reduces %EE by solubilizing drug in the continuous phase and promoting leakage. Increased water slightly improves EE by diluting free surfactant and enhancing interfacial packing. The negative Oil×Smix interaction shows that combined increases partially offset oil's effect, limiting EE gains. The response analysed by quadratic mixture design with model F = 8.95, $p < 0.05$, R^2 = 0.8703, Adj R^2 = 0,7730 indicating significant response. The actual and predicted values of Entrapment efficiency were correlated as shown in the figure 16.
Runs 4–6 (Oil ~20%, Smix 25–30%, Water 50–55%) define an optimal region yielding small PS (61–96 nm), low PDI (0.12–0.20), zeta −20 to −23 mV and high EE (84–87%). This composition balances droplet formation, stability and drug loading and should be refined via response surface optimization and experimental verification before scale-up.

3.9 Scanning electron microscopic study:
SEM was used to study the surface morphology of the resulting optimized NPs Annulation. The SEM images of the optimized formulations were shown in the figure 19 & 20.

3.10 Thermodynamic Stability:
The formulation showed robust short-term physical stability, no phase separation after three heating-cooling cycles (4°C↔45°C) or after 30 min centrifugation (3000 rpm) and no colour change on daily visual inspection. These results indicate strong interfacial stabilization and resistance to coalescence, longer-term stability testing is recommended to confirm shelf life.

3.11 Regression analysis:
Desirability-based optimization identified ideal formulation settings for the target responses. Regression analysis confirmed that the selected factors significantly influence CQAs. The optimized TCN nanoemulsion prepared using model-predicted settings showed responses closely matching predictions, validating the model and confirming the factors' combined impact on formulation performance.

3.12 Post-Optimization Analysis and Nanoemulgel Evaluation:
The optimized formulation showed excellent agreement between predicted and observed CQAs (PS 146.3 nm, PDI 0.228, zeta −28.4 mV, EE 84.5%), validating the regression model and desirability-based optimization.

3.13 Incorporation of TCN loaded NE into gel base:
The TCN nanoemulsion was incorporated into 0.5% Carbopol 934 gel, producing a homogeneous, spreadable, shear-thinning and bioadhesive matrix that preserved droplet size and entrapment, ensuring sustained local release while minimizing systemic exposure.

3.14 Evaluation of Nanoemulgel:

3.14.1 **Homegeneity:** The nanoemulgel showed homogeneous drug distribution, ensuring uniform dosing and minimizing local concentration gradients.
3.14.2 pH: pH was 5.6 ± 1.0, suitable for topical application and compatible with skin physiology

while preserving Carbopol stability and TCN integrity.

3.14.3 Spreadability: Spreadability (7.8 ± 0.02 cm) and shear-thinning viscosity enabled easy, uniform application and sustained residence at the site, preventing droplet coalescence.

3.14.4 Drug content: Drug content was 96.3 ± 0.5%, confirming minimal loss during processing and consistent dosing.

3.14.5 *In* Vitro Release and Kinetics: OPZ NEG demonstrated controlled, sustained release (0.03% at 0.5 h to 88.5% at 24 h figure 21) with minimal initial burst. Release fitted best to zero-order kinetics ($R^2 = 0.966$), indicating constant drug flux governed by Carbopol matrix diffusion, polymer relaxation/erosion and stable nanoemulsion droplet dispersion.

3.14.6 Permeability and flux: Steady-state flux (165 µg/cm²/h) and permeability (0.083 cm/h) confirmed efficient trans-membrane delivery. These results indicate that the nanoemulsion enhances drug thermodynamic activity and maintains availability at the membrane, enabling rapid local therapeutic concentrations with sustained exposure through zero-order release.

3.15 Stability:

Under accelerated conditions (40 ± 2 °C / 75 ± 5% RH), OPZ NE remained physically and chemically stable for 30 days, with negligible changes in appearance, pH and drug content, confirming formulation robustness.

3.16 Updated Risk Assessment:

FMEA showed high-risk factors were mitigated through targeted oil and Smix selection, Carbopol tuning and strict process controls. These measures ensured consistent nano-sized globules (<200 nm), low PDI (<0.3), stable zeta potential (±30 mV), controlled viscosity and reproducible drug release, effectively reducing formulation and stability risks and supporting further development of OPZ-NEG.

REFERENCES

1. Scott DL, Coulton BL, Symmons DP, Popert AJ. Long-term outcome of treating rheumatoid arthritis: results after 20 years. The Lancet. 1987 May 16;329(8542):1108-11.
2. Radu AF, Bungau SG. Management of rheumatoid arthritis: an overview. Cells. 2021 Oct 23;10(11):2857.
3. Kumari M, Sadhu P, Shah N, Talele C, Gohil D. Comprehensive Review Of Rheumatoid Arthritis: Insights, Challenges and Prospects. Journal of Advanced Zoology. 2024 Jan 1;45(1).
4. Guo Q, Wang Y, Xu D, Nossent J, Pavlos NJ, Xu J. Rheumatoid arthritis: pathological mechanisms and modern pharmacologic therapies. Bone research. 2018 Apr 27;6(1):15.
5. Rheumatol. 2019;71(1):1–20.
6. Tanaka Y, Yamaoka K. JAK inhibitors in rheumatoid arthritis: an evidence-based review. Immunol Rev. 2016;269(1):149–62.
7. Kekane KD, Bhavsar S. Tofacitinib: a novel Janus kinase inhibitor for rheumatoid arthritis. J Drug Deliv Ther. 2020;10(2):1–5.
8. Glynn LE. The chronicity of inflammation and its significance in rheumatoid arthritis. Annals of the Rheumatic Diseases. 1968 Mar;27(2):105.
9. Karnam S, Donthi MR, Reddy B, *et al.,* Recent innovations in topical delivery for RA. J Drug Deliv Sci Technol. 2024;82:104345.
10. Zou W, Fang Y, Xu D, Zhu Y. Increasing global burden of rheumatoid arthritis: an epidemiological analysis from 1990 to 2019.

Archives of Medical Science: AMS. 2023 Apr 9;19(4):1037.
11. Takanashi S, Kaneko Y. Unmet needs and current challenges of rheumatoid arthritis: difficult-to-treat rheumatoid arthritis and late-onset rheumatoid arthritis. Journal of Clinical Medicine. 2024 Dec 13;13(24):7594.
12. Valarmathy S, Devi Damayanthi R, Daisy Chella Kumari S, Surya S, Sri Vidhya P, Vaishnavi Durga GK. Nanoemulgel: A Comprehensive Review for Topical Drug Delivery. Int J Pharm Res (IJPPR). 2024;30(2):271–286.
13. Pramod K, Tahir MA, Charoo NA, Ansari SH, Ali J. Pharmaceutical product development: A quality by design approach. International journal of pharmaceutical investigation. 2016 Jul;6(3):129.
14. Sinha A, Garg U, Nagaich U, Chaudhary A, Pandey M, Jain N. Emulgels: a promising topical drug delivery system for arthritis management and care. Pharmaceutical Development and Technology. 2024 Jan 2;29(1):25-39.
15. Patel PA, Chaudhary SA, Mehta TA. Formulation and evaluation of self-nanoemulsifying drug delivery system of poorly soluble drug. J Pharm Sci Biosci Res. 2019;9(1):1–7.
16. Jaydip RM, Patel CN. Development and characterization of SNEDDS for enhancing oral bioavailability of poorly soluble drugs. Int J Pharm Sci Res. 2020;11(3):1200–8.
17. Aboul Fotouh K, Allam AA, El-Badry M. Development and optimization of self-nanoemulsifying drug delivery systems (SNEDDS) for improved oral absorption of poorly soluble drugs. Drug Dev Ind Pharm. 2017;43(4):603–12.
18. Daware S, Baiwar S, Warokar A, Somani K, Waghmare S, Agrawal S. An overview on structural and functional characterization of drug-excipient compatibility studies by FTIR, DSC, XRD and TGA. Res J Pharm Technol. 2025;18(3):1434–8. doi:10.52711/0974-360X.2025.00206.
19. Sivapriya S, Prabhakaran L, Venkatesan P. Evaluation of drug-excipient compatibility for Paroxetine nanoformulations using DSC and FTIR analysis. YMER. 2023;12(89):1–8.
20. Mendes E, Souto EB, Oliveira WP, Gremião MPD. Development of a self-nanoemulsifying drug delivery system (SNEDDS) for benznidazole: preliminary studies. Drug Dev Ind Pharm. 2017;43(4):661–9. doi:10.1080/03639045.2016.1266542.
21. Vohra A, Singh SK, Kumar R, Jain A, Jain SK. QbD-based development and optimization of self-nanoemulsifying drug delivery system (SNEDDS) of curcumin for enhanced therapeutic efficacy. Drug Dev Ind Pharm. 2017;43(6):909–19. doi:10.1080/03639045.2017.1291671.
22. Cornell JA. Experiments with mixtures: designs, models and the analysis of mixture data. 3rd ed. New York: Wiley-Interscience; 2011.
23. Kumar A, Saini R, Mishra LK, Anand A. Advancements in nanoemulgel formulation for enhanced topical drug delivery. ER Publications.
24. Jamadra M, et al. Preparation and evaluation of herbal gel formulation. Int J Pharm Sci Res. 2017;8(1):1–6.
25. Singh B, Kumar R, Ahuja N. Optimizing drug delivery systems using systematic “design of experiments.” Part II: Nanoemulsified topical gels of aceclofenac. Pharm Sci Tech. 2005;6(1):1–8.
26. Sharma A, Sharma US. Liposomes in drug delivery: progress and limitations. Int J Pharm. 1997;154(2):123–140.

27. Trotta M, Debernardi F, Caputo O. Preparation of solid lipid nanoparticles by a solvent emulsification-diffusion technique. Int J Pharm. 2003;257(1–2):153–160.
28. Jain S, Patel N, Lin S. Formulation and evaluation of nanoemulsion-based gel for topical delivery of celecoxib. Int J Pharm Sci Res. 2016;7(3):1234–1241.
29. Garg A, Ahmad MZ, Barkat MA, et al. Imaging techniques for characterization of nanoemulsions. In: Ahmad J, editor. Nanoemulsions in Health and Disease. CRC Press; 2022. p. 127–144.
30. Ghogare R, Waghmare S, Kamble H. Nanoemulsion–Characterisation Techniques and Formulation Methods. Int J Trend Sci Res Dev. 2022;6(3):638–647.
31. Bhardwaj A, Kanwar M. Evaluation of topical gel formulations of diclofenac sodium using different polymers. Asian J Pharm Clin Res. 2014;7(3):88–92.
32. Nayak BS, Nayak UK, Mohanty B. Formulation and evaluation of gel containing fluconazole. Int J PharmTech Res. 2010;2(1):105–108.
33. Basha BN, Prakasam K, Goli D. Formulation and evaluation of gel containing fluconazole-antifungal agent. Int J Drug Dev Res. 2011;3(4):109–128.
34. Patel RP, Patel NA, Patel KR, Patel NM. Formulation and evaluation of topical diclofenac sodium gel using different polymers. Int J Drug Dev Res. 2011;3(3):150–164.
35. Ramesh N, Kumar GP, Reddy MS. Formulation and evaluation of transdermal gels of ketoprofen using rat skin. J Pharm Sci Res. 2010;2(11):728–733.
36. Dash S, Murthy PN, Nath L, Chowdhury P. Kinetic modelling on drug release from controlled drug delivery systems. Acta Pol Pharm. 2010;67(3):217–223.
37. International Council for Harmonisation of Technical Requirements for Pharmaceuticals for Human Use. ICH Q1A(R2) Stability Testing of New Drug Substances and Products. 2003.

HOW TO CITE: Mohammad Noufal, Dr. Satheesha Babu B. K , Quality By Design Based Preparation and Evaluation of Topical Nanoemulgel Loaded with A Model Drug for Management of Rheumatoid Arthritis, Int. J. of Pharm. Sci., 2026, Vol 4, Issue 8, 4719-4751, https://doi.org/10.5281/zenodo.22144927

Tables

Table 1: Selected independent variables for optimization

COMPONENTS	NAME	UNITS	MIN	MAX
A	Amt of Oil	%	15	20
B	Amt of Smix	%	25	30
C	Amt of Water	%	50	55
			Total =	100.00

Table 2: Selected responses for optimization

RESPONSE	NAME	UNIT	GOAL
R1	Particle size	nm	Less than 200 nm
R2	PDI	-	Less than 0.3

R3	Zeta potential	mV	+/- 30mV
R4	Entrapment efficiency	%	More than 80%

Table 3: Formulation table for the preparation of nanoemulsion suggested by Design Expert software

Run	Amt of Oil	Amt of Smix	Amt of Water
	%	%	%
NE-1	17.5	30	52.5
NE-2	17.5	30	52.5
NE-3	15	30	55
NE-4	20	27.5	52.5
NE-5	20	27.5	52.5
NE-6	20	30	50
NE-7	17.5	27.5	55
NE-8	20	25	55

Table 4: Solubility data for screening of oils

Sl No	Oil	Absorbance at 286nm	Concentration (mcg/ml)
1	Olive	0.234	3.44
2	Isopropyl myristate	0.113	1.41
3	Eucalyptus	1.733	28.64
4	Oleic Acid	0.934	15.21
5	Peppermint	1.213	19.90

Table 5: Solubility data for screening of surfactants

Sl No	Surfactants	Absorbance at 286nm	Concentration (mcg/ml)
1	Tween 20	1.3	21.36
2	Tween 80	1.562	25.76
3	Poloxamer-188	0.834	13.53

Table 6: Solubility data for screening of co-surfactants

Sl No	Co-Surfactants	Absorbance at 286nm	Concentration (mcg/ml)
1	Transcutol®-P	2	33.12
2	PEG-400	1.7	28.08

Table 7: Emulsification efficiency test data

Sl no	Smix Ratio	Parameters

		%Transmittance	Emulsification Time	Phase separation
1	01:02	10	Less than 1 Min	Yes
2	01:01	75.4	Less than 1 Min	No
3	02:01	89.9	Less than 1 Min	No
4	2.5:01	91	Less than 1 Min	No
5	03:01	92.2	Less than 1 Min	No

Table 8: FT-IR spectra data

Functional Group	Expected Range (cm^{-1})	Pure TCN (cm^{-1})	Drug + Excipient Mixture (cm^{-1})
Hydrogen Bonding (O-H/ N-H)	3200 - 3400	3350	3356
Aliphatic (C-H) stretch	2850 - 2960	2920	2860
Carbonyl (C=O)	1650 - 1750	1747	1726
Aromatic (C=C)	1580 - 1600	1582	1594
Aliphatic Bending (CH_2)	1450 - 1460	1458	1458
Carboxylic Acid (COO)	1240 - 1260	1257	1249

Table 9: Aqueous titration data

AQUEOUS TITRATION (S_{MIX} in the Ratio 3:1)								
Oil: S_{MIX} Ratio	Smix (ml)	Oil (ml)	Water Added till Phase Change (ml)	Total	%Smix	%Oil	%Water	Appearance
02:08	0.4	1.6	0.7	2.7	14.8	59.3	25.9	Milky white
03:07	0.6	1.4	1.4	3.4	17.6	41.2	41.2	Milky white
04:06	0.8	1.2	2	4	20.0	30.0	50.0	Milky white
05:05	1	1	2.8	4.8	20.8	20.8	58.3	Bluish Transparent
06:04	1.2	0.8	3.3	5.3	22.6	15.1	62.3	Transparent
07:03	1.4	0.6	4.7	6.7	20.9	9.0	70.1	Transparent
08:02	1.6	0.4	4.8	6.8	23.5	5.9	70.6	Transparent
09:01	1.8	0.2	2.8	4.8	37.5	4.2	58.3	Transparent

Table 10: QTPP and CQA of TCN Nanoemulgel

QUALITY TARGETED PTODUCT PROFILE (QTPP) OF TCN NANO-EMULGEL			
QTPP ELEMENTS		**TARGET**	**JUSTIFICATION**
Dosage Form		O/W nano-emulsion (Later incorporated into gel base)	Enables solubilization & penetration of TCN for skin delivery
Route Of Administration		Topical	Avoids systemic side effects seen with oral TCN
Drug Release Profile		Sustained release more than 80% over 12 Hrs	Maintains therapeutic levels and reduces dosing frequency
Skin Penetration		Efficient permeation into inflamed joints	Critical for localized action in RA & nano-size enhances penetration
Therapeutic Indication		Rheumatoid arthritis management	Targets inflamed joints directly, improving efficacy and reducing toxicity
Appearance		Clear to Translucent, Low viscous & no phase separation	Indicates nano-size range and patient acceptability
Stability		Thermodynamically Stable under ambient & accelerated condition	Ensures shelf life and consistent performance
Critical Quality Attributes Of Drug Product	Viscosity	Less viscous & Easily spreadable	Facilitates topical application & Patient compliance
	pH	Skin compatible range (5-7)	Prevents skin irritation and stability
	Particle Size	Less than 200nm	Enhances skin permeation and physical stability
	Zeta Potential	+/- 30mV	Prevents coalescence and phase separation
	Polydispersity Index (PDI)	Less than 0.3	Ensures uniformity and reproducibility of formulation
	Emulsification Efficiency	% Transmittance NLT 80%	Ensures physical stability and aesthetic formulation
	Entrapment Efficiency	High (More than 80%)	Indicates effective drug loading and release control
	Drug Content	Accurate dosing (+/- 5%)	Ensures therapeutic consistency and regulatory compliance
	Invitro Drug Release	Sustained release more than 60% over 12 Hrs	Guides formulation tuning and therapeutic performance

Table 11: Initial Risk Assessment of formulation variables

Initial Risk Assessment for Formulation Variables (FMEA)				
Drug Product CQA	**Formulation Variables**			
	Oil Phase	**Surfactant Mixture**	**Aqueous Phase**	**Storage Condition**

Viscosity	High	High	Medium	Low
pH	Low	Medium	Medium	Low
Particle Size	Medium	High	Low	Low
Zeta Potential	Medium	High	High	Medium
Polydispersity Index (PDI)	Medium	High	Medium	Low
Entrapment Efficiency	High	High	Low	Low
Invitro Drug Release	High	High	Medium	Medium
Physical Stability	High	High	Low	Medium

Table 12: Justification for Initial Risk Assessment

INFLUENCED CQAs	FORMULATION VARIABLE	RISK PRIORITY	JUSTIFICATION
Viscosity	Oil Phase	High	Oil type and amount viscosity influence rheology and flow resistance (High-viscosity oils increase viscosity and low-viscosity oils yield lighter gels). The risk is high.
	Surfactant Mixture	High	Surfactants reduce interfacial tension and interact with gel matrix (Non-ionic surfactants may increase viscosity via steric stabilization, ionic surfactants alter electrostatic interactions). The risk is high.
	Aqueous Phase	Medium	Water content dilutes gel matrix, only higher water content reduces viscosity. The risk is medium.
	Storage Condition	Low	Elevated temperature reduces viscosity. The risk is low.
pH	Oil Phase	Low	Most pharmaceutical oils are chemically neutral and do not significantly alter pH. The risk is low.
	Surfactant Mixture	Medium	Surfactants types can influence pH through ionization or interaction with buffer systems. Selection of non-ionic surfactant and suitable mixture

			ratio can manage this. The risk is medium.
	Aqueous Phase	Medium	The aqueous phase is the primary carrier of pH. Buffer selection, ionic strength and water quality directly impact pH. The risk is medium.
	Storage Condition	Low	Under controlled conditions of temperature and light, nanoemulgels show good pH stability over time. However, extreme temperatures or prolonged exposure may cause hydrolysis or oxidation, which is rare but monitorable. The risk is low.
Particle Size	Oil Phase	Medium	Oil type and concentration influence droplet formation. Oils with high viscosity or poor emulsification may hinder size reduction. However, with proper selection of oil, it is manageable. The risk is medium.
	Surfactant Mixture	High	Surfactants are critical for reducing interfacial tension and stabilizing droplets. Improper Smix ratio, surfactant type, or concentration can lead to coalescence, polydispersity, or phase separation. The risk is high.
	Aqueous Phase	Low	Typically composed of purified water or buffer, the aqueous phase has minimal direct impact on particle size. The risk is low.
	Storage Condition	Low	Same justification as mentioned for pH.
Zeta Potential	Oil Phase	Medium	Oils generally have low inherent charge, when oils interact with surfactants or co-surfactants, potentially altering zeta potential and emulsion stability. The risk is medium.
	Surfactant Mixture	High	Surfactants directly affect zeta potential by forming charged layers around droplets. Improper Smix ratio can destabilize the system, leading to aggregation or phase separation. The risk is high.
	Aqueous Phase	High	The aqueous phase determines ionic strength and pH, both of which critically affect zeta potential. Water purity can alter the electrical double layer around droplets. It has direct role in electrostatic stabilization. The risk is high.

	Storage Condition	Low	Same justification as mentioned for pH.
Polydispersity Index (PDI)	Oil Phase	Medium	Same justification as mentioned for particle size.
	Surfactant Mixture	High	Same justification as mentioned for particle size.
	Aqueous Phase	Medium	The aqueous phase affects PDI indirectly through pH, ionic strength. The risk is medium.
	Storage Condition	Low	Same justification as mentioned for pH.
Entrapment Efficiency	Oil Phase	High	Entrapment efficiency is highly dependent on the drug's solubility in the oil phase. Oils with poor solubilizing capacity may lead to low EE%. Selecting the right oil is critical for maximizing drug loading and retention within droplets. The risk is high.
	Surfactant Mixture	High	Surfactants stabilize the oil-water interface and influence drug partitioning. Improper Smix ratio may cause drug leakage into the aqueous phase or micelle formation, reducing EE%. High surfactant concentration can also compete with oil for drug solubilization. The risk is high.
	Aqueous Phase	Low	The aqueous phase has minimal direct impact on EE%, The risk is low.
	Storage Condition	Low	Same justification as mentioned for pH.
Invitro Drug Release	Oil Phase	High	The oil phase governs drug solubility and partitioning. If the oil has poor drug affinity or high viscosity, it can hinder diffusion from droplets into the gel matrix and across the skin barrier. The risk is high.
	Surfactant Mixture	High	Surfactants influence droplet size, interfacial tension and drug release kinetics. Improper Smix ratio may lead to micelle formation or drug leakage into the aqueous phase, altering release profiles. High surfactant levels can also disrupt skin lipids, affecting permeation. The risk is high.
	Aqueous Phase	Medium	Improper aqueous phase may reduce gel consistency or alter drug release kinetics. The risk is medium.

	Storage Condition	Medium	IVDR can be affected by temperature-induced changes in droplet size, viscosity and drug stability. The risk is medium.
Physical Stability	Oil Phase	High	The oil phase significantly affects droplet size, viscosity and zeta potential. Oils with poor compatibility or high viscosity can lead to phase separation, coalescence, or Ostwald ripening over time. The risk is high.
	Surfactant Mixture	High	Same justification as mentioned for particle size.
	Aqueous Phase	Low	The aqueous phase plays a minimal role in destabilization. It mainly serves as the continuous phase and contributes to gel consistency. The risk is low.
	Storage Condition	Medium	Nanoemulgels are generally stable under room temperature and elevated temperature (40 ± 2°C), but mechanical stress can reveal hidden instabilities, prolonged exposure to low temperatures (4 ± 2°C) may induce Ostwald ripening. The risk is medium.

🔴 **High Risk = Requires immediate optimization and control**
🟡 **Medium Risk = Monitor closely during development**
🟢 **Low Risk = Standardize but less critical to formulation failure**

Table 13: Physical characterization of NE

Formulation Code	Colour	Phase Separation	Transmittance %
NE-1	Yellowish Transparent	No	92.5
NE-2	Yellowish Transparent	No	93
NE-3	Transparent	No	98
NE-4	Bluish Transparent	No	97
NE-5	Bluish Transparent	No	96
NE-6	Transparent	No	98

NE-7	Yellowish Transparent	No	98
NE-8	Yellowish Transparent	No	96

Table 14: Results obtained for Particle size, PDI, Zeta potential and %EE

Formulation Code	Particle Size (nm)	PDI	Zeta Potential (mV)	%EE
NE-1	153	0.35	-31	83.64
NE-2	157	0.32	-35	84.04
NE-3	146	0.23	-27	85.32
NE-4	89	1	-17	81.99
NE-5	90	0.96	-15	84.34
NE-6	84	1	-22	80.71
NE-7	160	0.77	-13	83.44
NE-8	61	1	-19	87.07

Table 15: Actual VS predicted results

Variables	Predicted	Actual
Particle Size	150.5 nm	145.3 nm
PDI	0.225	0.228
Zeta Potential	-27.98 mV	-28.4 mV
%EE	85.8%	84.5%

Table 16: Evaluation parameter for OPZ-NE

Sl no	Evaluation Parameter	Result
1	Colour	Yellowish Transparent
2	Phase separation	No

3	% Transmittance	98±2%
4	Drug content	97±1.5%

Table 17: Thermodynamic stability data of OPZ-NE

Test	Condition applied	Duration	Observation	Result
Heating- Cooling Cycles	4°C ↔ 45°C alternating every 24 h	3 cycles (6 days)	No phase separation	Stable
Centrifugation test	3000rpm	30 min	No phase separation	Stable
Visual inspection	Ambient temperature	Daily	No colour change	Stable

Table 18: Evaluated parameters for OPZ-NE

PARAMETERS	RESULTS
Homogeneity	Homogenous drug distribution
pH	5.6 ± 1.0
Spreadability	7.8 ± 0.02 cm
Viscosity	1073 cps
Drug content	95.3 ± 0.5 %

Table 19: In vitro drug release data of OPZ-NEG

USP Type-II Dissolution apparatus Using Egg Membrane			
Sl No	Time(Hr)	CDR	%CDR
1	0	0.0000±0.0000	0.00±0.00
2	0.5	0.0006±0.0001	0.03±0.01
3	1	0.0193±0.0002	1.00±0.50
4	2	0.0997±0.0009	5.14±0.55
5	4	0.1849±0.0012	9.53±1.12
6	6	0.4402±0.0023	22.69±1.5
7	8	0.6688±0.0055	34.48±2.5
8	12	1.1665±0.0112	60.13±2.0
9	24	1.7172±0.0368	88.52±1.5

Table 20: In vitro drug release kinetics data

	Zero order	First order	Higuchi	Korsmeyer – Peppas
K_{Slope}	0.5190	-0.0385	24.074	1.2348

R^2	0.966	0.9539	0.9649	0.963

Table 21: In Vitro Permeability Study

Steady-State Flux	**165 µg/cm²/h**
Permeability Coefficient	**0.083cm/h**

Table 22: Stability studies data of OPZ-NE

Storage Condition: 40.0 ± 2.0 °C / 75.0 ± 5.0% RH				
Sample Type	**Sampling Interval**	**Appearance**	**pH**	**Drug Content**
OPZ-NE	0 Day	Translucent	5.6±0.2	95.3±0.5%
	7 Day	Translucent	5.6±0.5	95.2±0.5%
	15 Day	Translucent	5.5±0.2	95.0±0.5%
	22 Day	Translucent	5.5±0.2	95.0±0.5%
	30 Day	Translucent	5.5±0.2	95.0±0.5%

Table 23: Updated Risk Assessment of formulation variables

Updated Risk Assessment for Formulation Variables (FMEA)				
Drug Product CQA	**Formulation Variables**			
	Oil Phase	**Surfactant Mixture**	**Aqueous Phase**	**Storage Condition**
Viscosity	Low	Low	Medium	Low
pH	Low	Medium	Medium	Low
Particle Size	Medium	Low	Low	Low
Zeta Potential	Medium	Low	Low	Medium

Polydispersity Index (PDI)	Medium	Low	Medium	Low
Entrapment Efficiency	Low	Low	Low	Low
Invitro Drug Release	Low	Low	Medium	Medium
Physical Stability	Low	Low	Low	Medium

Table 24: Justification for updated Risk Assessment of formulation variables

FORMULATION VARIABLE	INFLUENCED CQAs	JUSTIFICATION
Oil Phase	Viscosity	Rheological studies confirm that the viscosity is within the desired range for topical application. The risk is reduced from high to low.
	Entrapment Efficiency	Entrapment efficiency is consistently high (>80%) , indicating robust drug loading and minimal leakage. The risk is reduced from high to low.
	IVDR	IVDR profiles show sustained release with no burst effect, aligning with therapeutic goals for RA. The risk is reduced from high to low.
	Physical Stability	Accelerated and real-time stability studies show no signs of phase separation, creaming, or degradation. The risk is reduced from high to low.
Surfactant Mixture	Viscosity	Rheological studies confirm that the viscosity is within the desired range for topical application. The risk is reduced from high to low.
	Particle Size	Achieved nano-range globule size (<200 nm). The risk is reduced from high to low.
	Zeta Potential	Zeta potential values are within ±30 mV. The risk is reduced from high to low.
	Polydispersity Index (PDI)	PDI < 0.3 confirms uniform particle distribution and homogeneity. The risk is reduced from high to low.
	Entrapment Efficiency	High entrapment (>80%) achieved through optimized formulation. The risk is reduced from high to low.
	Invitro Drug Release	Follows zero-order kinetics with sustained release profile. The risk is reduced from high to low.
	Physical Stability	No phase separation, creaming, or degradation. The risk is reduced from high to low.
Aqueous Phase	Zeta Potential	Zeta potential values are within ±30 mV. The risk is reduced from high to low.

Figures

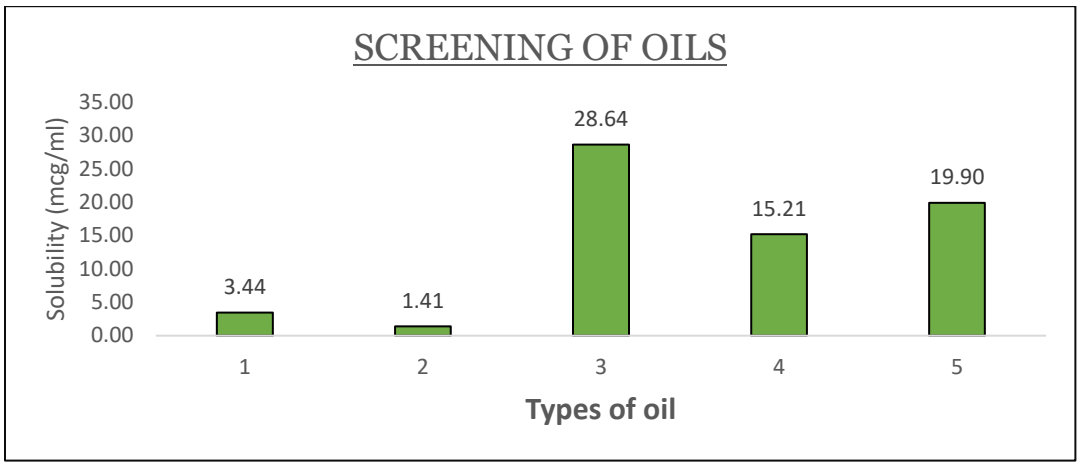

Figure 1: Solubility graph for screening of oils (1=Olive oil; 2=Isopropyl myristate; 3=Eucalyptus oil; 4=oleic acid; 5=Peppermint oil)

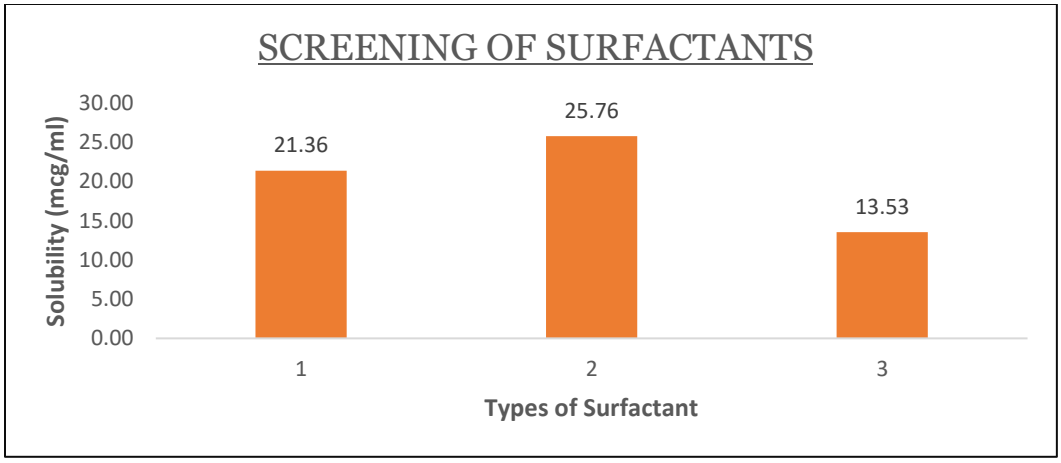

Figure 2: Solubility graph for screening of surfactants (1=Tween20; 2=Tween80; 3=Poloxamer-188)

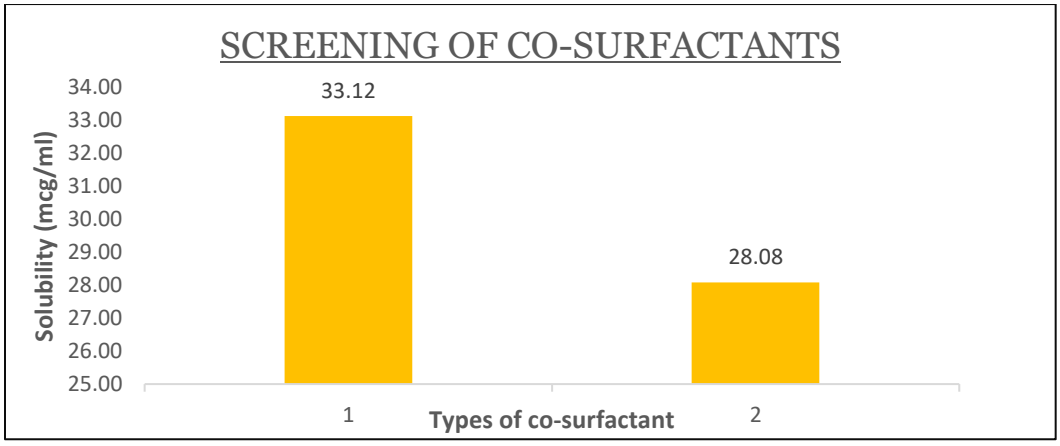

Figure 3: Solubility graph for screening of co-surfactants (1= Transcutol®-P; 2= PEG-400)

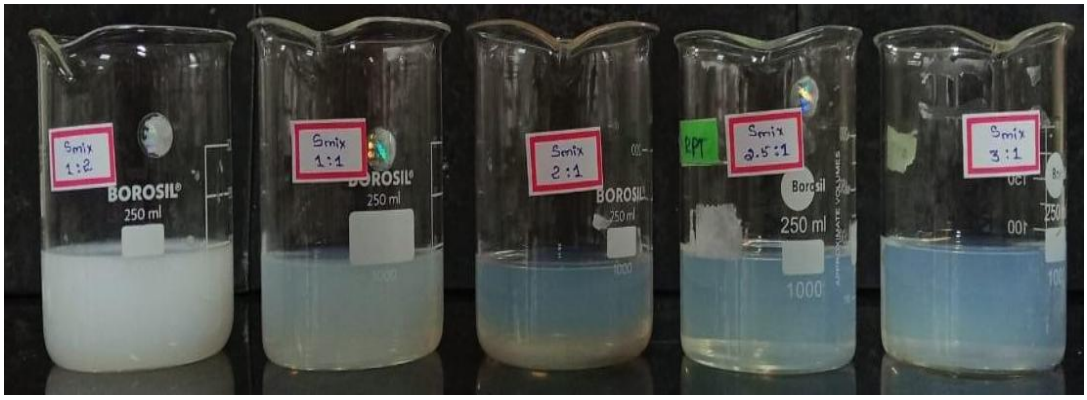

Figure 4: Pictorial Representation for Visual Inspection of different Smix ratio

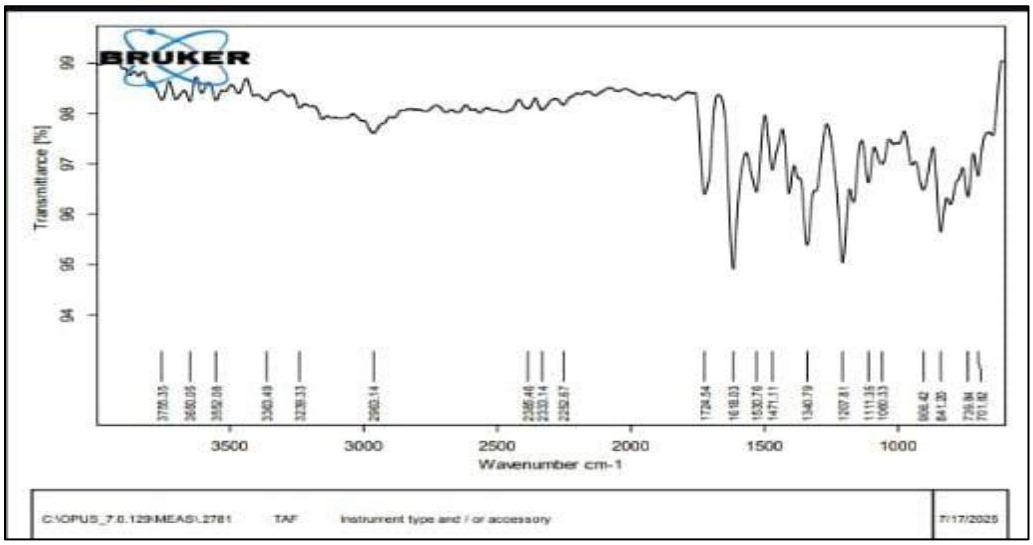

Figure 5: FTIR spectra of pure TCN

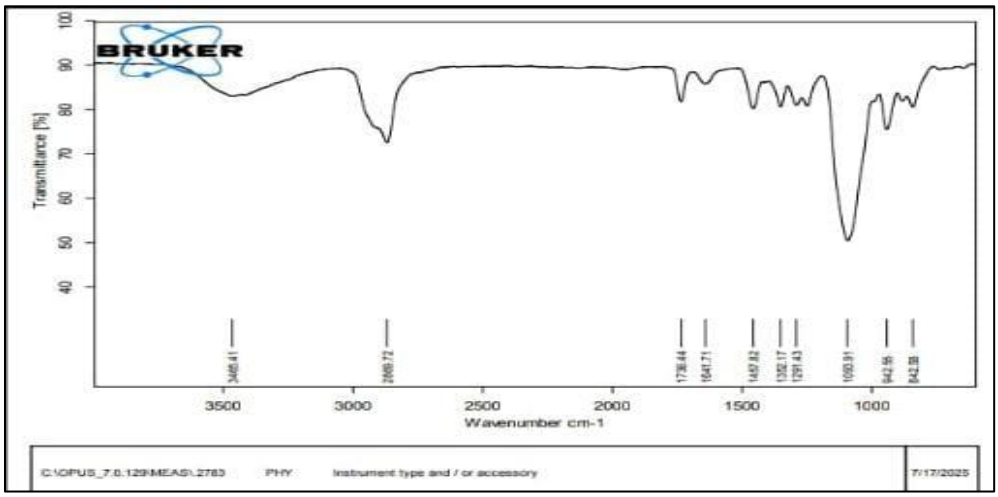

Figure 6: FTIR spectra of TCN + excipients

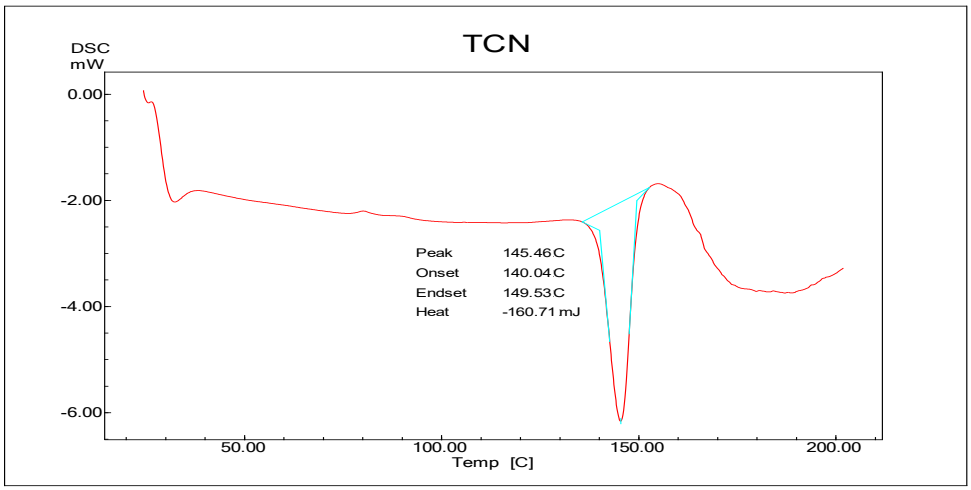

Figure 7: DSC thermograph of pure TCN drug

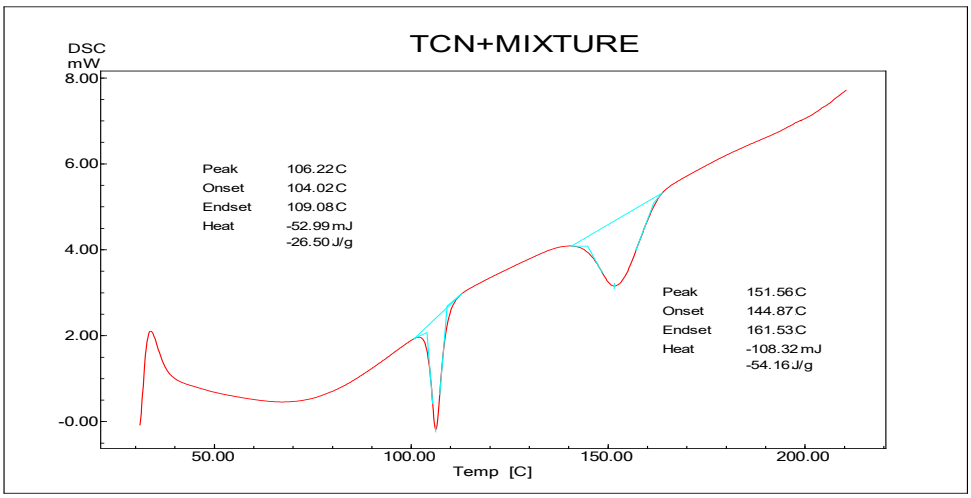

Figure 8: DSC thermograph of TCN + excipients

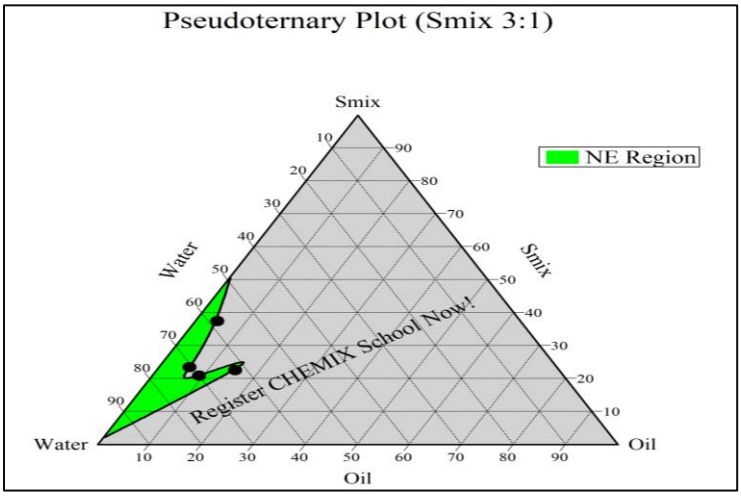

Figure 9: Pseudo ternary phase diagram

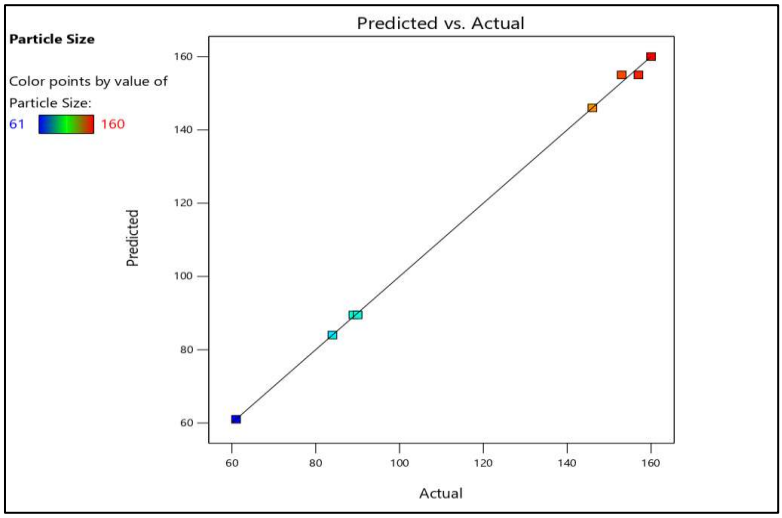

Figure 10: Actual vs Predicted correlation of Particle size

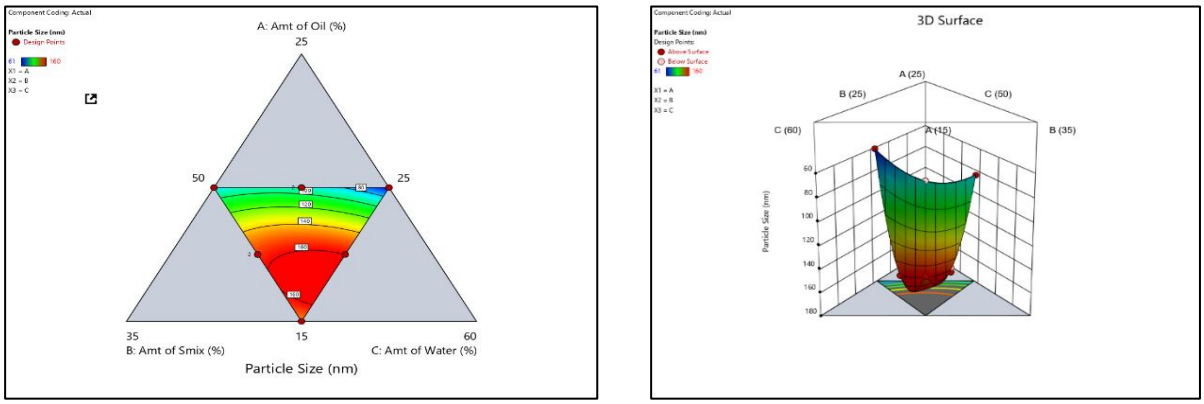

Figure 11: Model graph a) Contour and b) 3D surface of Particle size

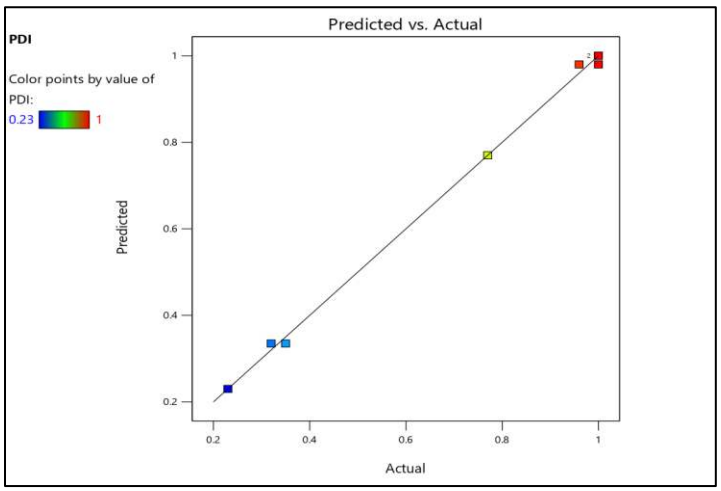

Figure 12: Actual vs Predicted correlation of PDI

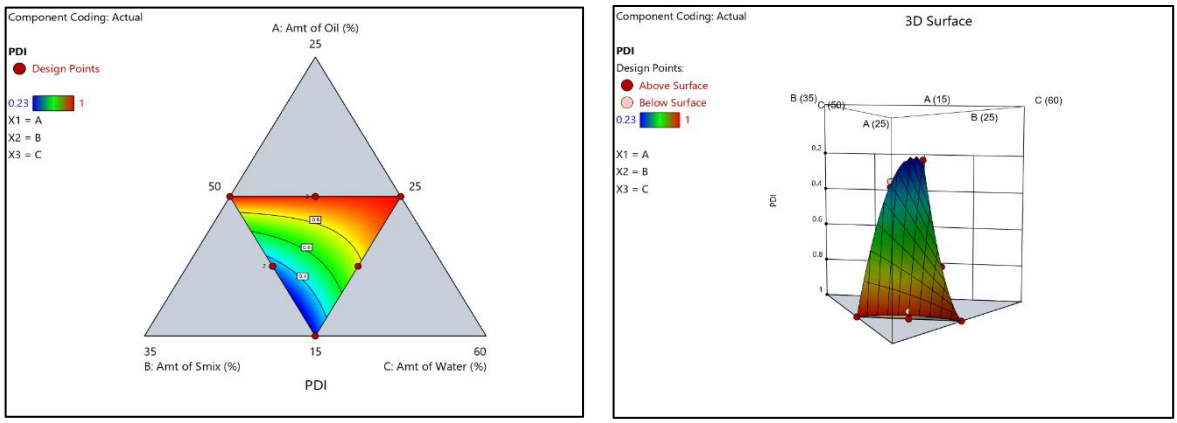

Figure 13: Model graph a) Contour and b) 3D surface of PDI

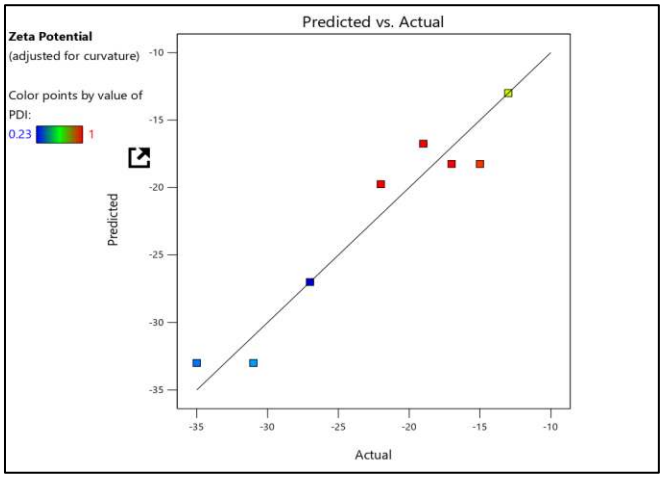

Figure 14: Actual vs Predicted correlation of Zeta potential

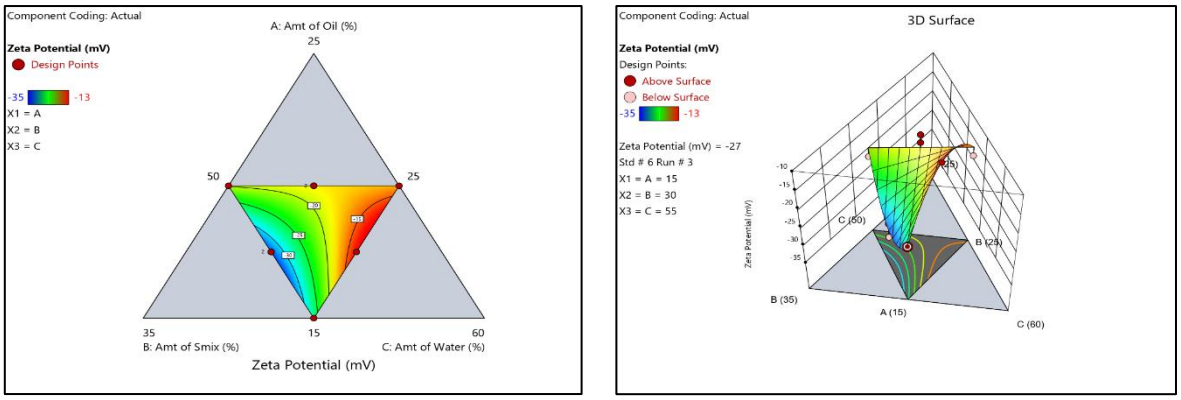

Figure 15: Model graph a) Contour and b) 3D surface of Zeta Potential

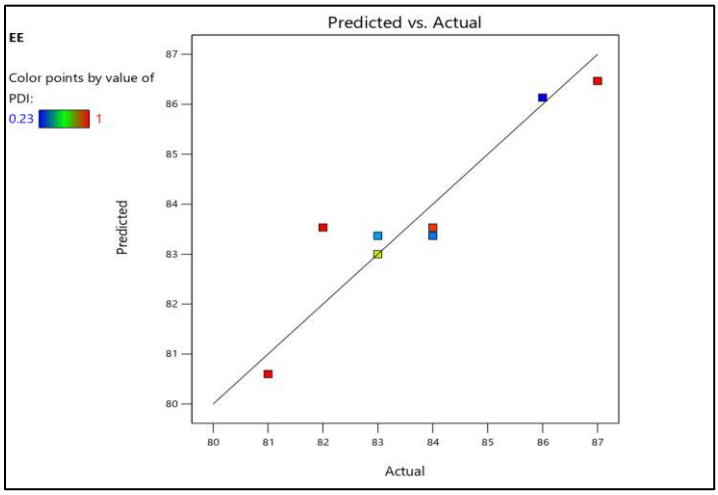

Figure 16: Actual vs Predicted correlation of %EE

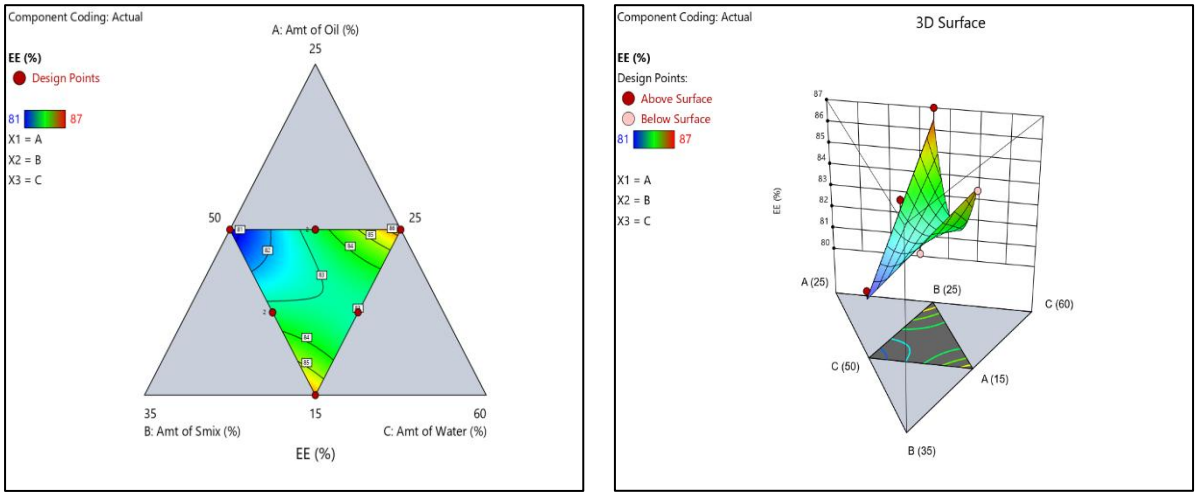

Figure 17: Model graph a) Contour and b) 3D surface of %EE

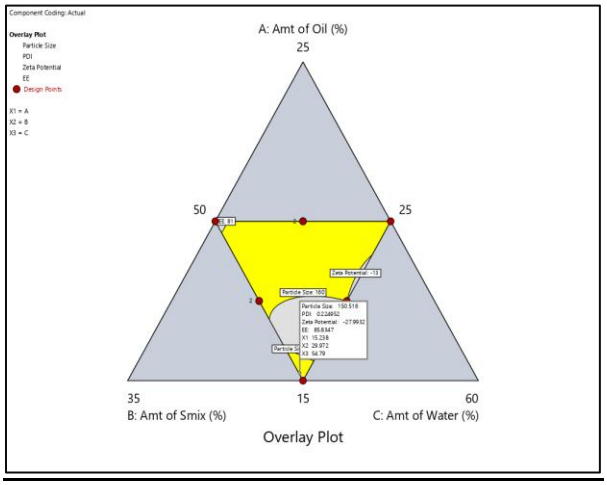

Figure 18: Overlay plot (Design Space)

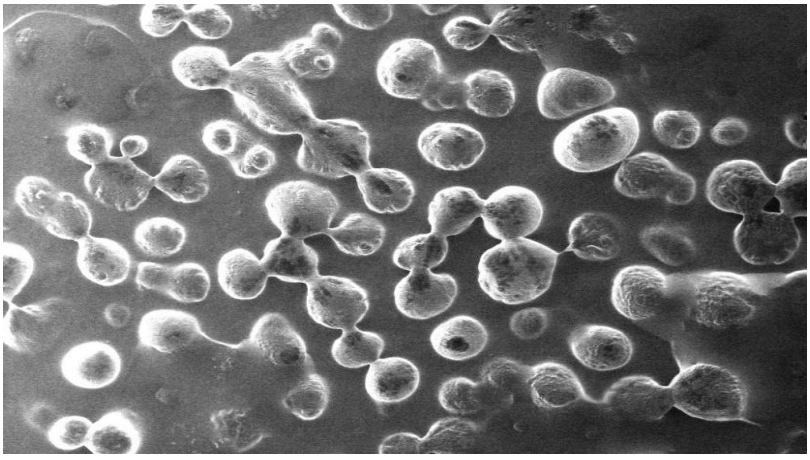

Figure 19: SEM image of OPZ-NEG

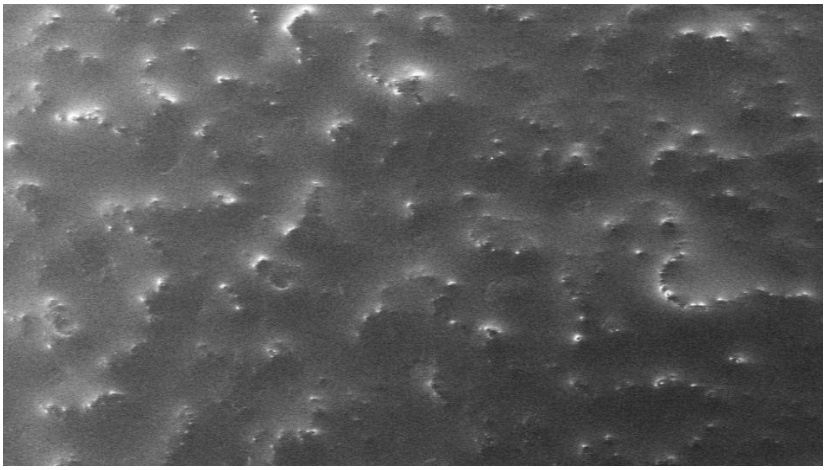

Figure 20: SEM image of OPZ-NEG

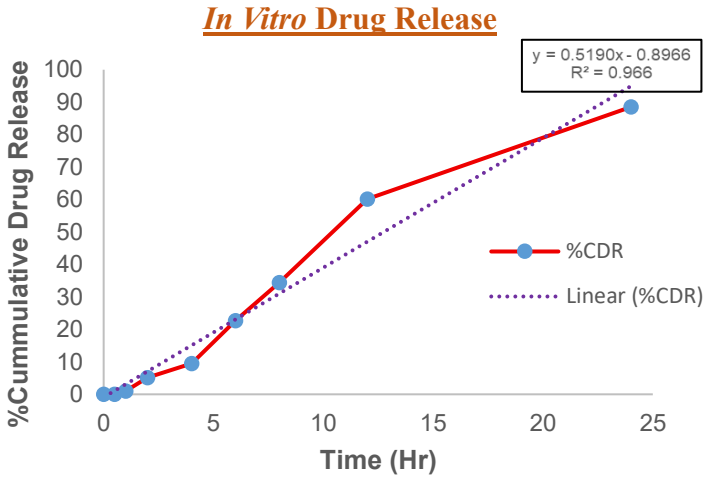

Figure 21: In vitro drug release profile of OPZ-NEG